Original Article

Interference with connective tissue growth factor attenuated fibroblast-to-myofibroblast transition and pulmonary fibrosis

Zhizhou Yang[1,2#], Mengmeng Wang[1,2#], Liping Cao[1#], Rui Liu[1], Yi Ren[1], Liang Li[1], Yuhao Zhang[2], Chao Liu[1], Wei Zhang[1], Shinan Nie[1,2]^, Zhaorui Sun[1,2]^

[1]Department of Emergency Medicine, Jinling Hospital, Medical School of Nanjing University, Nanjing, China; [2]Department of Emergency Medicine, The First School of Clinical Medicine, Southern Medical University, Nanjing, China

Contributions: (I) Conception and design: Z Yang, M Wang, L Cao, Z Sun, S Nie; (II) Administrative support: Y Ren, W Zhang; (III) Provision of study materials or patients: R Liu, L Li; (IV) Collection and assembly of data: Z Yang, M Wang, Y Zhang; (V) Data analysis and interpretation: C Liu, W Zhang; (VI) Manuscript writing: All authors; (VII) Final approval of manuscript: All authors.

[#]These authors contributed equally to this work.

Correspondence to: Prof. Shinan Nie; Prof. Zhaorui Sun. Department of Emergency Medicine, Jinling Hospital, Medical School of Nanjing University, Zhongshan East Road 305, Nanjing 210002, China. Email: shn_nie@sina.com; sunzhr84@163.com.

Background: The aberrant activation and phenotype shift of resident fibroblasts in lung tissues via fibroblast-to-myofibroblast transition (FMT) is considered a pivotal step in pulmonary fibrogenesis, resulting in excessive extracellular matrix (ECM) production and deposition. However, the molecular mechanisms regulating FMT and lung fibrosis are still unclear. Connective tissue growth factor (CTGF) has been reported to be both an ECM protein and a versatile signaling molecule that is involved in multiple pathophysiological contexts, especially fibrosis. The relationship between CTGF, FMT, and lung fibrosis has not yet been well defined.

Methods: In this study, a pulmonary fibrosis (PF) rat model and FMT cell model induced by paraquat (PQ) were established to explore the relevant regulatory mechanisms *in vivo* and *in vitro*.

Results: The results showed that the CTGF was highly activated and was a mediator of canonical Wnt signaling during FMT and PF. The inhibition of the CTGF by small-interfering ribonucleic acid decreased the expression of FMT markers, including α-smooth muscle actin, vimentin, and collagen I, inhibited the activated Wnt signaling pathway, and ameliorated lung fibrosis.

Conclusions: Our findings showed that CTGF was the key effector of the FMT and fibrotic changes, and emphasized the therapeutic potential of the inhibitor or monoclonal antibody against CTGF for PF.

Keywords: Connective tissue growth factor (CTGF); fibroblast-to-myofibroblast transition (FMT); Wnt/β-catenin signaling; small-interfering RNA (siRNA); pulmonary fibrosis (PF)

Submitted Mar 04, 2022. Accepted for publication Apr 13, 2022.
doi: 10.21037/atm-22-1397
View this article at: https://dx.doi.org/10.21037/atm-22-1397

Introduction

Pulmonary fibrosis (PF) is an uncommon but severe long-term complication of novel coronavirus severe acute respiratory syndrome coronavirus 2 (SARS-CoV-2) infection, and has attracted significant attention and research interest (1,2). However, the molecular mechanisms of PF development remain unclear, and to date, no effective therapeutic approaches have been developed. In recent decades, both the incidence and mortality of PF have increased significantly all around the world (3). Typical pathological changes of PF include the excessive production

^ ORCID: Shinan Nie, 0000-0002-9989-4766; Zhaorui Sun, 0000-0002-8969-498X.

and deposition of the extracellular matrix (ECM), tissue remodeling, and stiffening, which can be induced by multiple risk factors, including definite and unknown causes (4). In addition to genetic predispositions and aging, the imbalance of damage and repair often result in the scarring of lung tissues when exposed to hazardous materials.

Historically, bleomycin has been the most extensively used agent in PF model induction, and its pulmonary toxicity is widely recognized (5). In previous studies, another toxin, the paraquat (PQ, also known as methyl viologen) has also often been adopted to induce PF models owing to its good reproducibility (6,7). Currently, PQ is still one of the most commonly used herbicides (plant killers) worldwide, is quick to act and has a low environmental impact. Many PQ poisoning cases caused by accident or suicide have been reported. The main cause of death after poisoning is progressive PF induced by the accumulated PQ, which is actively absorbed by the polyamine uptake system in the lung (8,9). It should be noted that the development and progression of PF caused by various hazardous substances, including bleomycin, PQ, asbestos, and fine particulate matter (PM2.5, aerodynamic diameter ≤2.5 μm), share some common pathological characteristics (10,11). The molecular mechanisms behind PQ-induced PF in the current study could provide a reference for other PF models and potential intervention targets for poisoning.

Myofibroblasts are the dominant collagen-producing cells during lung fibrogenesis, which mainly originate from resident fibroblasts via fibroblast-to-myofibroblast transition (FMT) (12). Research on this pivotal transition should elucidate the elaborate process of fibrogenesis. Connective tissue growth factor (CTGF, also known as CCN2), a cysteine-rich, secreted ECM protein, was initially discovered in endothelial cells and fibroblasts, and can activate fibroblasts (13). Compared to other organs and tissues, CTGF expression has been shown to be higher in blood vessels and the lungs, and to participate in their development and disorders. Additionally, there is accumulating evidence that CTGF is also a versatile signaling and regulatory molecule involved in multiple biological and pathological processes, including cell proliferation, angiogenesis, wound healing, tissue fibrosis, and tumor development (14,15). In fibrotic tissue, the high expression of CTGF can be induced by many cytokines, the most notable of which is transforming growth factor beta (TGF-β). In addition, CTGF may also increase the expression of different cytokines, including TGF-β, resulting in positive feedback loops (16). Other cytokines, such as vascular endothelial growth factor and integrin, have also been reported to interact with CTGF (16).

However, the mechanisms underlying CTGF are not yet fully understood. Notably, CTGF was recently found to be able to bind to the low-density lipoprotein receptor-associated protein (LRP), which is one of the main receptors of Wingless/Int-1 (Wnt) ligands (17). The canonical Wnt signaling pathway has been shown to be associated with tissue repair and fibrosis (18). In a previous study, we found that CTGF was increased and affected the cellular function of lung fibroblasts when stimulated by PQ, but the relationship between CTGF, FMT and PF was not well defined, and the downstream signaling and in-depth mechanism of CTGF regulating FMT were not revealed (19).

In this study, a PF rat model and a FMT cell model were established both *in vivo* and *in vitro* to investigate the regulatory roles of CTGF on PQ-induced FMT and PF, and the therapeutic potential of the small-interfering ribonucleic acid (siRNA) against CTGF was also examined. We present the following article in accordance with the ARRIVE reporting checklist (available at https://atm.amegroups.com/article/view/10.21037/atm-22-1397/rc).

Methods

Experimental animals

A total of 60 adult male Sprague-Dawley (SD) rats (aged 8–10 weeks and weighing 200–220 g) without specific pathogen were obtained from the Experimental Animal Center of Nanjing University and were maintained in a 12-h light-dark cycle (25±1 ℃, 50–60% humidity) with free access to standard chow and water. At the end of the experiment, all the rats were sacrificed by cervical dislocation. Sodium pentobarbital (Sigma-Aldrich, USA) was used intraperitoneally (50 mg/kg, i.p.) for anaesthetization, and efforts were made to alleviate any pain. The current protocol was prepared before the study without registration. All animal experiments were performed under a project license (No. 2019JLHGKJDWLS-035) granted by Institutional Ethics Committee of Jinling Hospital, Medical School of Nanjing University, in compliance with institutional guidelines for the care and use of animals.

Animal grouping and PF model establishment

The 60 SD rats were randomly divided into the following

5 groups using a random-number table: (I) the control group (n=12): the rats were administered intraperitoneally with sterile saline; (II) the PF model group induced by PQ (also referred to as the PQ group) (n=12): the rats were administered with PQ (20 mg/kg, i.p.); (III) the LV-NC group (n=12): the rats were administered (i.p.) with sterile saline and received the intratracheal treatment of lentivirus vector expressing negative control; (IV) the PQ group (n=12): the rats were administered with PQ (20 mg/kg, i.p.) and received the intratracheal administration of lentivirus vector expressing negative control; (V) the PQ + CTGF-siRNA group (n=12): the rats were administered with PQ (20 mg/kg, i.p.) and received intratracheal administration of lentivirus vector expressing siRNA against CTGF, which was established by Genechem (Shanghai, China).

Cell culture and treatment

The human fetal lung fibroblast cell line (MRC-5) was purchased from the American Type Culture Collection (ATCC, (USA) and was cultured in high-glucose Dulbecco's Modified Eagle's Medium (DMEM) with 10% (v/v) fetal bovine serum (FBS; Gibco, USA) and 1% (v/v) penicillin/streptomycin (Invitrogen, CA, USA) and incubated at 37 ℃ in a 5% carbon dioxide (CO_2) humidified incubator. The culture medium was replaced every 72 h, and the cells were passaged at a 1:3 ratio every 3–4 days. The siRNA targeting CTGF messenger RNA (mRNA) and non-targeting control siRNA were purchased from Genechem (Shanghai, China). For the transfection, Lipofectamine RNAiMAX Reagent and Opti-MEM (Invitrogen, CA, USA) were used in accordance with the manufacturer's instructions. All the MRC-5 cells were collected and analyzed 72 h after transfection.

Histological examination

Briefly, the rat lung specimens were collected, fixed in 4% buffered paraformaldehyde for 24 h, embedded in paraffin, and sectioned to 5 μm-thick slices by freezing microtome. Next, the tissue sections were deparaffinized, hydrated, and stained with hematoxylin and eosin (H&E) (Beyotime, Shanghai, China) and the Modified Masson's Trichrome stain kit (Solarbio, Beijing, China). The histological examination was performed by 2 independent pathologists blinded to the study protocol. The wet/dry (W/D) weight ratio was determined to assess the degree of pulmonary edema following PQ administration. In brief, the wet weight was measured after excising the lung tissues, and the lung was then placed in an oven until the weight remained constant, at which time it was weighed again to measure the dried weight. The W/D weight ratio was calculated by dividing the dry weight by the wet weight. A hydroxyproline (HYP) detection kit (Jiancheng, Nanjing, China) was used to measure the HYP content of rat lungs to assess the lung collagen deposition.

Electrophoresis and Western blotting

Total proteins were extracted from tissues and cells in ristocetin-induced platelet aggregation buffer (Beyotime, China) containing a protease inhibitor (Roche, USA) and phosphatase inhibitor cocktail (Sigma-Aldrich, USA). Protein concentration was measured by a Pierce Bicinchoninic Acid Protein Assay Kit (Thermo Fisher Scientific, USA). After separation by 10% or 12% sodium dodecyl sulphate polyacrylamide gels, the proteins were then electrophoretically transferred onto polyvinylidene fluoride membranes (Millipore, Germany). After incubation with 5% bovine serum albumin (BSA) for blocking, the membranes were then incubated with primary antibodies at 4 ℃ overnight. After being washed 3 times, the membranes were incubated with secondary antibodies at 37 ℃ for 1 h. The protein bands were visualized using the enhanced chemiluminescence detection kit (Merck, Germany). Representative images were captured by the Tanon 5200 Chemiluminescent Imaging System (Tanon, China), and the band intensities were determined by the Image J Software (version 1.41).

Immunofluorescence analysis for tissues and cells

For the tissue immunofluorescence staining, a 10-μm thick section was fixed in acetone at 4 ℃ for 15 min, and then blocked with 5% BSA containing 0.4 % Triton X-100 and incubated for 30 min at room temperature. After incubation with primary antibodies at 4 ℃ overnight, the tissue slides were incubated with fluorescence (Alexa Fluor 488 or 594)-conjugated secondary antibodies (Invitrogen, USA) in the dark for 1 h at room temperature. Next, the tissue slides were incubated with 1 μg/mL 4',6-diamidino-2-phenylindole (DAPI; Thermo Scientific, USA) for nuclear labeling. For the cell immunofluorescence staining, the cells were fixed by 4% paraformaldehyde for 10 min. After blocking with PBS containing 10% FBS, the cells were then incubated with primary antibodies at 4 ℃

overnight. After being rinsed 3 times with PBS with 0.2% Triton X-100, the cells were incubated with fluorescence-conjugated secondary antibodies (Invitrogen, USA) in the dark for 1 h. All the samples were observed under a confocal fluorescence microscope (Olympus, Shinjuku, Japan).

Immunohistochemical staining

In brief, 5-μm thick tissue sections were deparaffinized, rehydrated, and immersed in 3% hydrogen peroxide reagent to block the endogenous peroxidase activity. After blocking with 5% BSA at room temperature for 1 h, the tissue slides were then incubated with specific primary antibodies at 4 ℃ overnight. After being washed 3 times, the sections were then incubated in horseradish peroxidase–conjugated secondary antibody (Boster, China) in the dark for 30 min at room temperature. The immunoreaction was revealed with 3,3'-Diaminobenzidine (Sigma, USA) as a substrate and examined under Leica DM750 system (Leica Microsystems, Germany).

Arterial blood gases

To assess the lung function of the rats, arterial blood gas was determined by the G3+ i-STAT test cartridges and i-STAT 1 blood analyzer (Abbott, USA) in accordance with the manufacturer's instructions. Briefly, 80–100 μL arterial blood was obtained from the rat left ventricle, and then added to the sample well for the analyses. Next, 2 main arterial blood gas parameters, including the partial pressure of oxygen (PaO_2, mmHg) and partial pressure of carbon dioxide ($PaCO_2$, mmHg), in the arterial blood were recorded and compared among the different groups.

Statistical analysis

All the experimental data are presented as the mean ± standard deviation (mean ± SD). The data were subjected to analysis using SPSS software (Version 23.0; IBM Corp, USA) and GraphPad Prism 7.0 (GraphPad Software Inc., USA). Differences between the 2 groups were compared using the Student's *t*-test, and a one-way analysis of variance with Dunnett's post-hoc test was used to compare multiple groups. A 2-tailed $P<0.05$ was considered statistically significant.

Results

CTGF was upregulated in the lung tissues of rats administered PQ

The histopathological examination of the lung tissues of rats in different groups was conducted 14 and 28 days after the PQ challenge using H&E staining and Masson's trichrome staining. The lung tissues of the rats in the PQ group showed disrupted microscopic structures, inflammatory cell infiltration, epithelial damage, collagen production, and deposition, while the lungs of the rats in the Control group maintained a relatively normal appearance (*Figure 1A*,*1B*). Compared to the Control group, the HYP content and W/D ratio of the lungs of the rats in the PQ group were significantly increased ($P<0.05$; *Figure 1C*,*1D*). To further confirm the development of tissue fibrosis at the molecular level, a variety of epithelial markers (occluding and E-cadherin) and mesenchymal markers [α-smooth muscle actin (α-SMA), vimentin, and collagen I] were detected by immunofluorescence, immunohistochemistry, and Western blotting. The expression levels of occluding and E-cadherin were decreased in the PQ group, while the expression of α-SMA, vimentin and collagen I were significantly elevated ($P<0.05$; *Figure 2*). Additionally, the expression of CTGF, β-catenin, and Wnt1-inducible signaling pathway protein 1 (WISP1) were also enhanced in the lungs of the rats in the PQ group as determined by Western blotting (*Figure 2C*,*2D*). The above-mentioned results confirmed PF development and indicated that CTGF was upregulated and the canonical Wnt signaling pathway was activated during fibrotic changes caused by PQ.

CTGF promoted the FMT of MRC-5 cells treated with PQ

When treated with PQ (50 μmol/L) for 3 days, the expression of α-SMA, vimentin, and collagen I was increased in the MRC-5 cells (see *Figure 3A*). Additionally, the expression of CTGF and the downstream molecules of Wnt signaling pathway (β-catenin and WISP1) in the PQ-treated MRC-5 cells were highly upregulated (see *Figure 3A*,*3B*). To confirm the effects of CTGF on the MRC-5 cells, recombinant CTGF (rCTGF, 100 ng/mL) was used in the subsequent experiments. Similar to the results for the rats treated with PQ, the expression levels of the FMT markers, such as α-SMA, vimentin, and collagen I, were also elevated in rCTGF-treated MRC-5 cells as detected by immunofluorescence and Western blotting

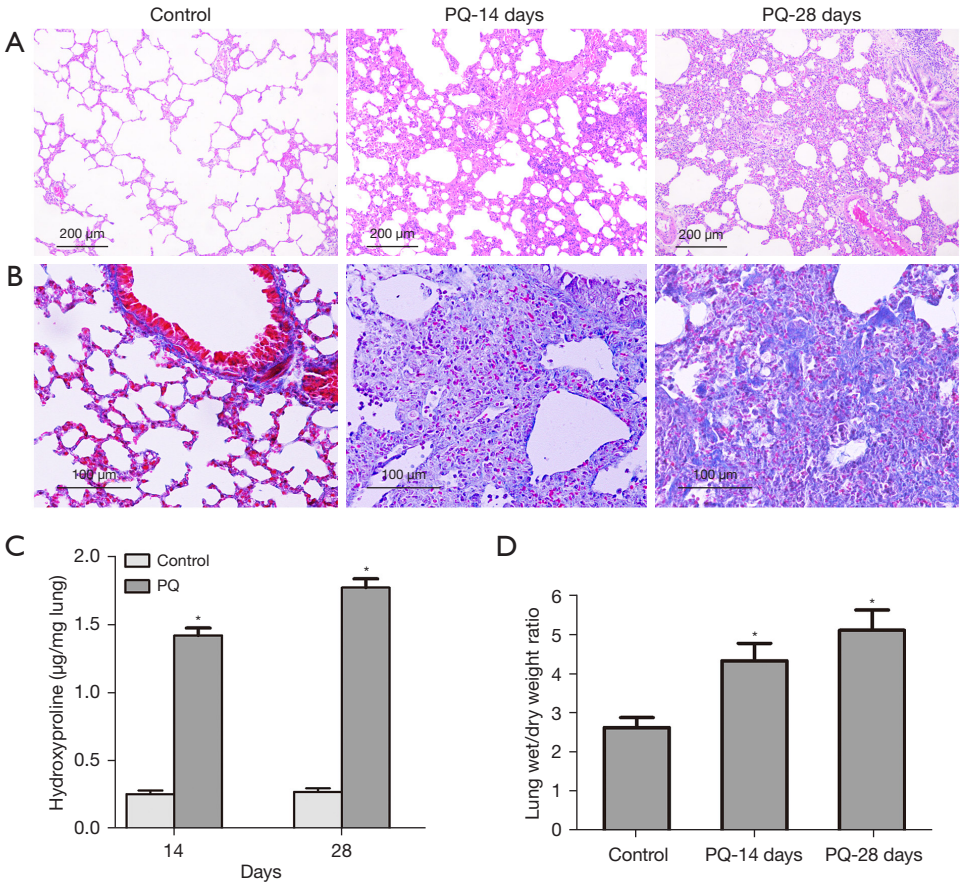

Figure 1 PF was induced by PQ. The rats in the Control group and PQ group were administered either saline or PQ (20 mg/kg). Fibrosis was evaluated by H&E staining (A, ×100), Masson's trichrome staining (B, ×200). Hydroxyproline content (C) and the W/D weight ratio (D) of lung tissue were determined. *, P<0.05 *vs.* Control group. PF, pulmonary fibrosis; PQ, paraquat; H&E, hematoxylin and eosin; W/D, wet/dry.

(see *Figure 3C,3D*). Notably, β-catenin and WISP1, the important signaling molecules of Wnt signaling pathway were also upregulated in the rCTGF-treated MRC-5 cells (see *Figure 3C,3D*).

Suppression of CTGF inhibited the PQ-induced transition of MRC-5 cells

The above-mentioned results indicated that the FMT of MRC-5 cells was induced by PQ and CTGF. RNAi technology was used to further elucidate the roles of CTGF on the transition of MRC-5 cells caused by PQ. The expression of CTGF was downregulated (see *Figure 4A*), and the expression of upregulated FMT markers, including α-SMA, vimentin, and collagen I were also suppressed 3 days after transfection (see *Figure 4A,4B*). Notably, the high expression levels of β-catenin, cycin D1 and WISP1 in the PQ-treated MRC-5 cells were also inhibited when CTGF was knocked down by siRNA (see *Figure 4A*).

Interference with CTGF detained the development of PF in vivo

To further investigate the roles of CTGF in PQ-induced FMT and PF *in vivo*, CTGF-siRNA was applied intratracheally in the rat models. After 28 days, the histological appearance as presented by H&E staining and Masson's trichrome staining (see *Figure 5A,5B*), the HYP content (see *Figure 5C*), and the W/D ratio (see *Figure 5D*) of the lung tissues of the rats were examined. Lung injury, edema, collagen deposition, and fibrosis caused by PQ were alleviated due to interference with CTGF expression. Several pulmonary function indices of rats in the PQ + CTGF-siRNA group were also improved. Compared to the

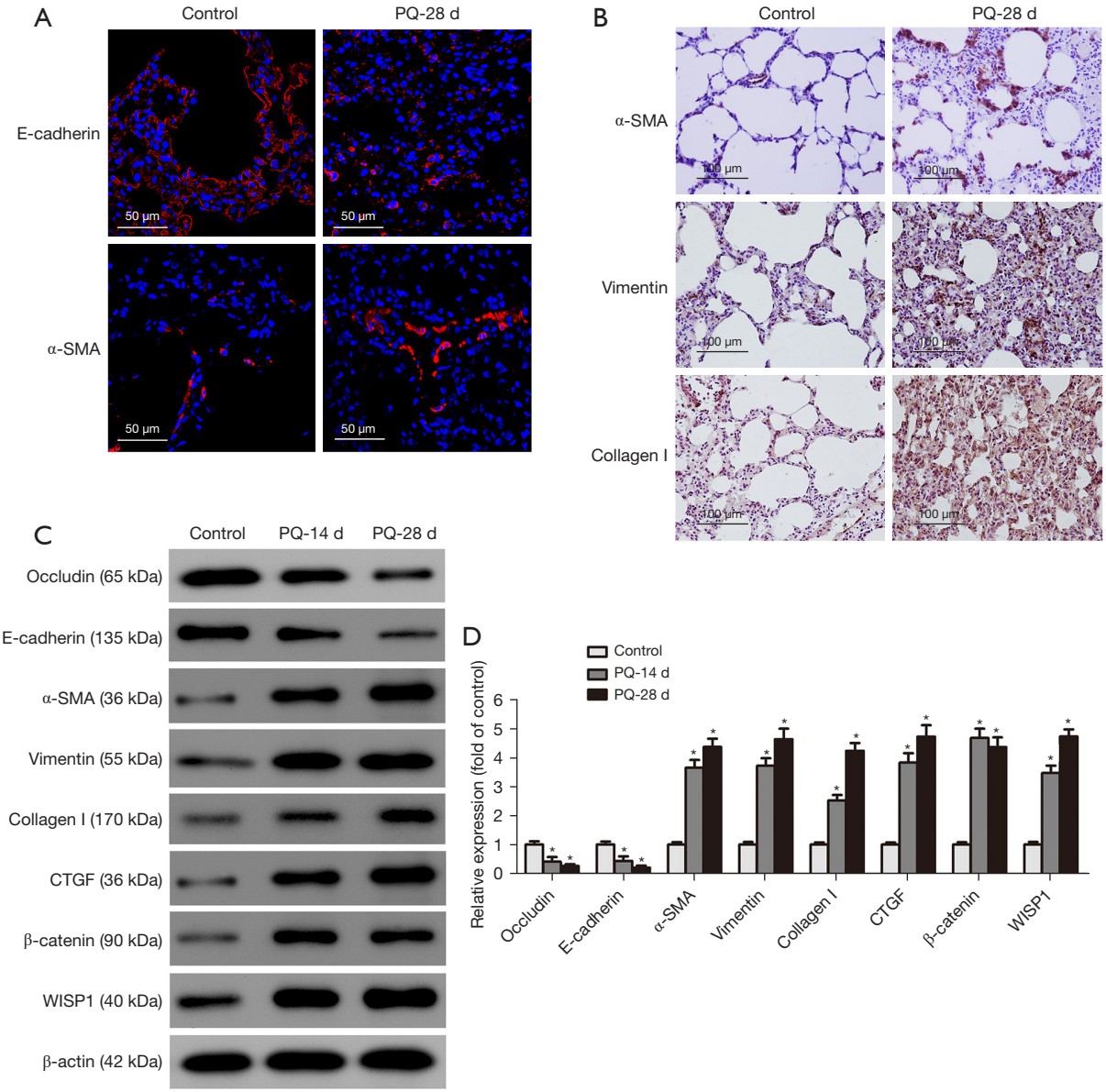

Figure 2 CTGF was upregulated in the lung tissues of rats in the PQ group. The location and expression of E-cadherin and α-SMA were detected by immunofluorescence (A, ×600); the expression of α-SMA, vimentin, and collagen I were determined by immunohistochemistry (B, ×200); the expression changes of occludin, E-cadherin, α-SMA, vimentin, collagen I, CTGF, β-catenin and WISP1 were assessed by Western blotting (C) and normalized to β-actin (D). *, P<0.05 *vs.* Control group. CTGF, connective tissue growth factor; PQ, paraquat; α-SMA, α-smooth muscle actin.

PQ group, interference with CTGF increased PaO_2 and decreased $PaCO_2$ (see *Figure 5E,5F*; P<0.05).

Compared to the PQ-treated rats, the expression levels of FMT markers α-SMA, vimentin, and collagen I were significantly decreased in the lungs of rats in the PQ + CTGF-siRNA group (see *Figure 5G,5H*). Additionally, along with the inhibition of CTGF, the expression of β-catenin, cyclin D1, and WISP1 were also downregulated in the lungs of rats in the PQ + CTGF-siRNA group (see *Figure 5G,5H*).

Discussion

During the past decades, PF has represented a huge

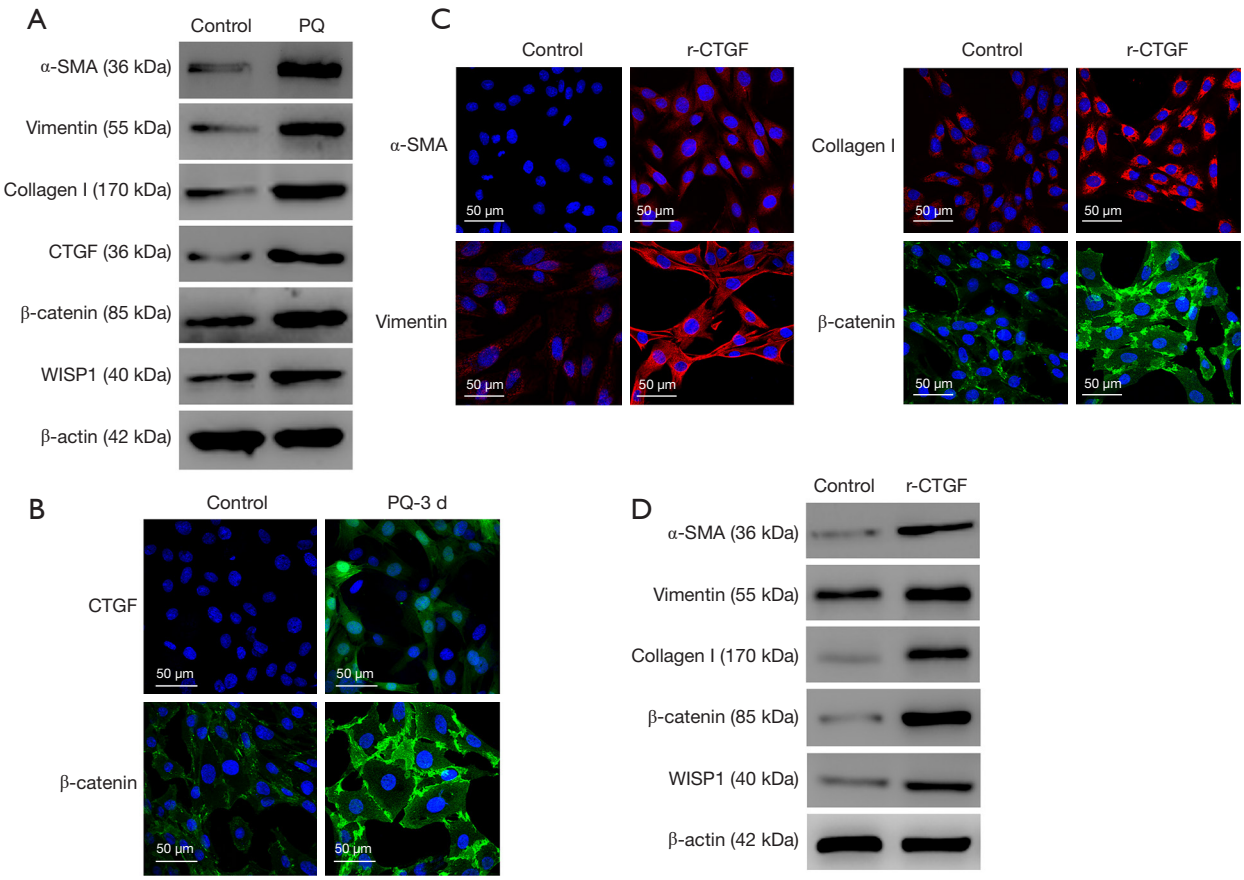

Figure 3 CTGF was upregulated and promoted FMT in PQ-treated MRC-5 cells. (A) After being treated with PQ (50 μmol/L) for 3 days, the expression changes of α-SMA, vimentin, collagen I, CTGF, β-catenin, and WISP1 in the MRC-5 cells were determined by Western blotting; (B) the expression levels of CTGF and β-catenin in the MRC-5 cells were further determined by immunofluorescence (×600); (C) after being treated with r-CTGF (recombinant CTGF, 100 ng/mL), the expression and location of α-SMA, vimentin, collagen I, and β-catenin in MRC-5 cells were detected by immunofluorescence (×600), and the expression of α-SMA, vimentin, collagen I, β-catenin, and WISP1 were also determined by Western blotting (D). CTGF, connective tissue growth factor; FMT, fibroblast-to-myofibroblast transition; PQ, paraquat; α-SMA, α-smooth muscle actin.

burden for families and societies, especially in the context of the COVID-19 pandemic. The harsh reality is that most patients are doomed to experience lung dysfunction, subsequent respiratory failure, and ultimately death. However, 2 anti-fibrotic medications (pirfenidone and nintedanib) have been reported to slow down the progressive process and preserve pulmonary function (20).

Acute lung injury and subsequent PF caused by different risk factors, including PQ, usually presented shared characteristics, including the proliferation, activation and FMT of fibroblasts (21). As the activated state of fibroblasts and other precursor cells, myofibroblasts originally exert the roles of repairing lost or damaged ECM proteins, which are important for restoring tissue integrity (12,22). However, the excessive activation, dysregulated timing, and spatial coordination of pro-fibrotic signals and a series of inflammatory factors lead to the excessive production and accumulation of stiff collagenous ECM, and subsequently fibrosis and the dysfunction of organs. In addition to TGF-β1, several new factors have recently been found to promote FMT, including muscle blind-like 1 (MBNL1) and long non-coding RNA SNHG1 (lncSNHG1) (23,24).

The roles of CTGF/CCN2 in a variety of fibrotic disorders should be highlighted, as previous studies have reported that it is a pro-fibrotic factor, biomarker, and potential target (25-27). In carbon tetrachloride–induced

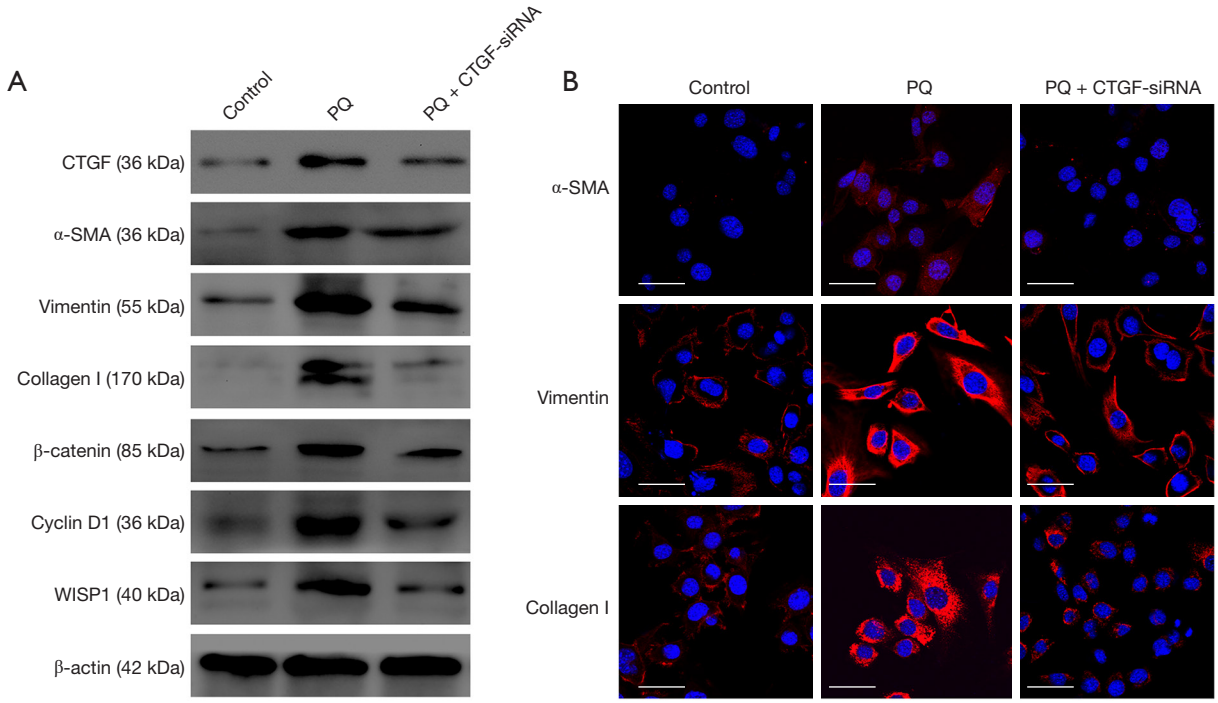

Figure 4 The suppression of CTGF inhibited PQ-induced FMT. (A) The expression changes of CTGF, α-SMA, vimentin, collagen I, β-catenin, cyclin D1, and WISP1 in the MRC-5 cells were determined Western blotting; (B) the expression levels of α-SMA, vimentin and collagen I in the MRC-5 cells were also determined by immunofluorescence (×600). CTGF, connective tissue growth factor; FMT, fibroblast-to-myofibroblast transition; PQ, paraquat; α-SMA, α-smooth muscle actin.

liver fibrosis and congenital hepatic fibrosis, CTGF has been shown to be essential for fibrogenesis and could be a new therapeutic target for blocking the progression (28,29). In chronic kidney disease, CTGF was shown to increase the phosphorylation levels of LRP6 and glycogen synthase kinase-3β, induce nuclear β-catenin accumulation, and induce the epithelial-to-mesenchymal transition of tubular epithelial cells, resulting in renal fibrosis (30-32).

A new research has confirmed the synergistic effect of CTGF and TGF-β1 (33). Intriguingly, single nucleotide polymorphisms (SNPs) in CTGF have been found to associate with the process of PF (34). In the current study, CTGF was highly upregulated in PQ-induced PF, which promoted the transition of MRC-5 cells both *in vivo* and *in vitro*. Notably, canonical Wnt signaling pathway was also activated by PQ and rCTGF, and the important roles of Wnt/β-catenin signaling in organ development, wound healing, and tissue fibrosis have been well established previously (18,35). Thus, CTGF may promote FMT and PF by activating the Wnt signaling pathway, and some co-receptors and signaling feedback loops might be involved. However, in the nucleus pulposus, the activation of Wnt/β-catenin was reported to decrease the expression of CTGF mRNA and protein involving the mitogen-activated protein kinase (MAPK) pathway (36). Such results indicate that the regulatory relationships between CTGF, the Wnt/β-catenin, and other signaling pathways might harbor tissue-specificity or organ-specificity.

We also investigated the application potential of CTGF-siRNA in our study. Our findings suggest that the blockage of CTGF expression suppresses the FMT and detains the development of PF induced by PQ. Recently, Dorn *et al.* showed that fibroblast-derived CTGF modulates fibrosis in the heart and that inhibiting CTGF induction in activated fibroblasts is sufficient to abrogate the cardiac fibrotic response to angiotensin II (37). Thus, interfering with CTGF could represent a promising therapeutic strategy.

Inhibitors for CTGF have been developed for the treatment of organ fibrosis. A fully recombinant human monoclonal antibody against CTGF, pamrevlumab (FG-3019), has been enrolled in a phase-3 trial, due to its safety,

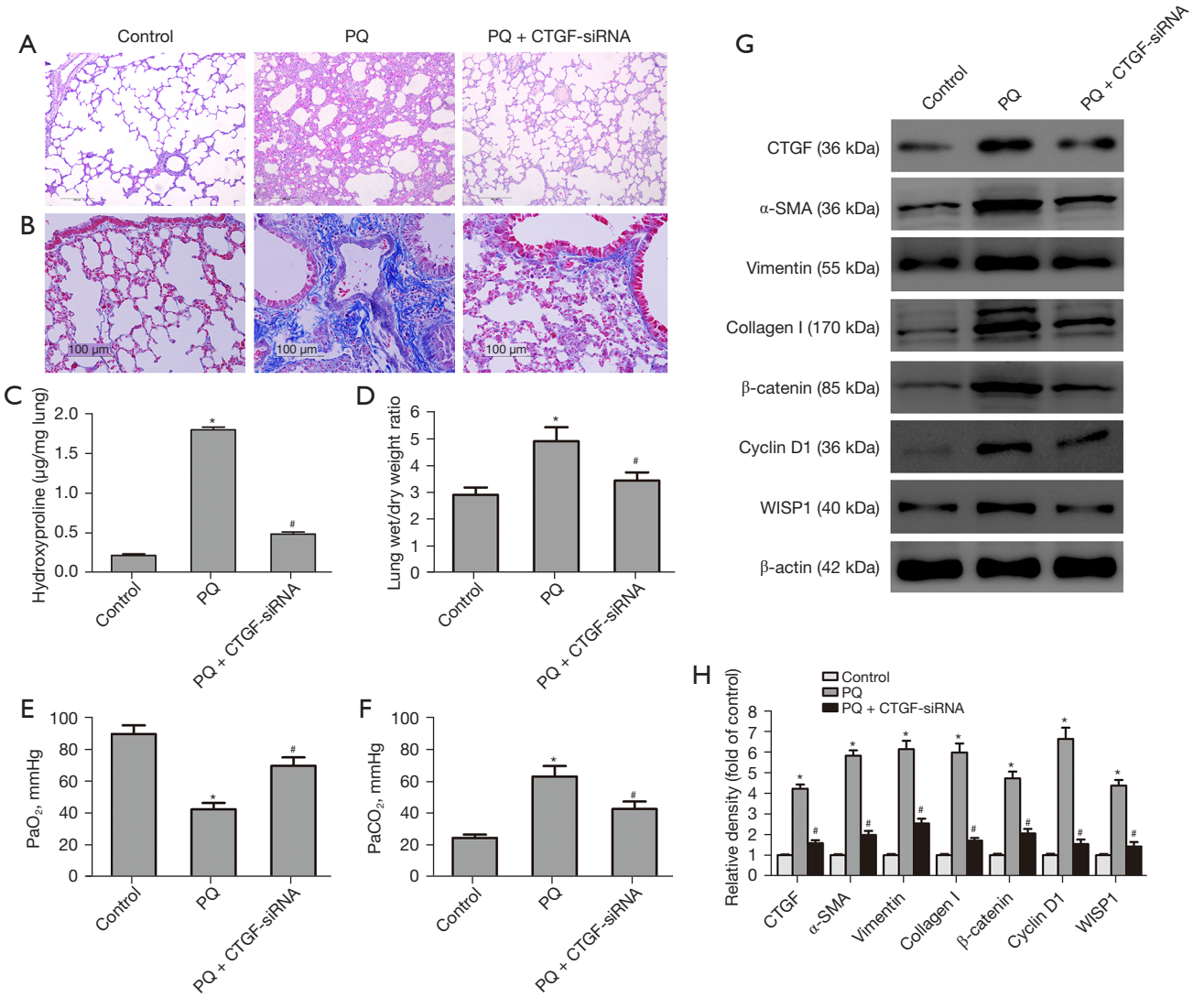

Figure 5 Interfering with CTGF detained PF *in vivo*. Lung fibrosis was evaluated by H&E staining (A, ×100), Masson's trichrome staining (B, ×200). Hydroxyproline content (C), and the W/D weight ratio (D). The PaO_2 (E) and $PaCO_2$ (F) in the arterial blood were measured. The expression protein levels of CTGF, α-SMA, vimentin, collagen I, β-catenin, cyclin D1, and WISP1 in the rat lung tissues were determined by Western blotting (G) and normalized to the expression of β-actin (H). *, P<0.05 *vs.* Control group. #, P<0.05 *vs.* PQ group. CTGF, connective tissue growth factor; PF, pulmonary fibrosis; PQ, paraquat; α-SMA, α-smooth muscle actin; H&E, hematoxylin and eosin; W/D, wet/dry; PaO_2, partial pressure of oxygen; $PaCO_2$, partial pressure of carbon dioxide.

tolerability, and efficacy at attenuating the progression of idiopathic PF (38,39). Notably, blocking CTGF using pamrevlumab was shown to reduce skeletal muscle fibrosis, indicating that the monoclonal antibody could be a pan-anti-fibrotic agent (40). In addition, whether there are some specific lnRNAs and miRNAs that can regulate CTGF signaling and PF remain to be explored. Further research also needs to be conducted to determine whether this antibody could be used to treat lung fibrosis induced by COVID-19, PQ, PM2.5, or other factors.

As *Figure 6* shows, CTGF was identified as a pivotal mediator of the regulatory network involved in the PQ-induced FMT and PF both *in vitro* and *in vivo*. CTGF, along with the activated canonical Wnt signaling and other relevant pathways, plays an important role in the phenotype shift of lung fibroblasts and fibrotic changes. Inhibitors

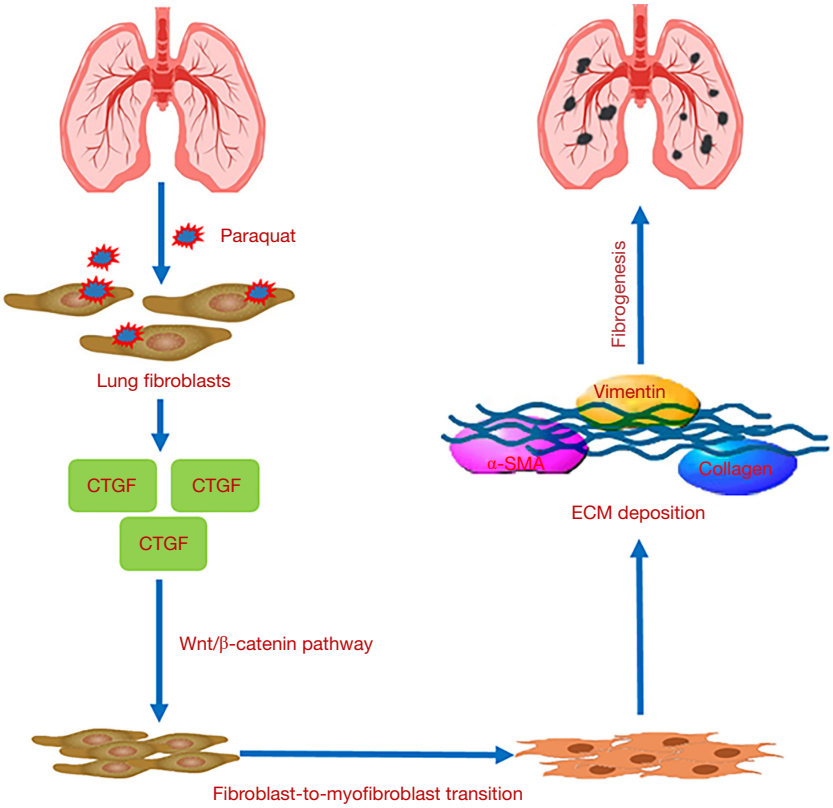

Figure 6 Schematic diagram of the regulatory roles of CTGF on the FMT of lung fibroblasts and PF. CTGF was increased by PQ stimulation, which subsequently promoted the FMT of lung fibroblasts, ECM production and deposition, and ultimately PF. CTGF, connective tissue growth factor; FMT, fibroblast-to-myofibroblast transition; PF, pulmonary fibrosis; PQ, paraquat; ECM, excessive extracellular matrix.

targeting the CTGF have the therapeutic potential to ameliorate the progressive lung fibrosis.

Acknowledgments

Funding: This work was supported by the National Natural Science Foundation of China (Nos. 82172182, 82102311, 81701894 and 81401583); the Natural Science Foundation of Jiangsu Province (Nos. BK20190247 and BK20211136); the Science Foundation of Jiangsu Health Commission (No. H2018039); the China Postdoctoral Science Foundation (Nos. 2018M643890 and 2020M683718); and the Jiangsu Postdoctoral Research Foundation (Nos. 2018K048A and 2020Z193).

Footnote

Reporting Checklist: The authors have completed the ARRIVE reporting checklist. Available at https://atm.amegroups.com/article/view/10.21037/atm-22-1397/rc

Data Sharing Statement: Available at https://atm.amegroups.com/article/view/10.21037/atm-22-1397/dss

Conflicts of Interest: All authors have completed the ICMJE uniform disclosure form (available at https://atm.amegroups.com/article/view/10.21037/atm-22-1397/coif). The authors have no conflicts of interest to declare.

Ethical Statement: The authors are accountable for all aspects of the work in ensuring that questions related to the accuracy or integrity of any part of the work are appropriately investigated and resolved. This study was approved by the Institutional Ethics Committee of Jinling Hospital, Medical School of Nanjing University (No. 2019JLHGKJDWLS-035), in compliance with institutional

guidelines for the care and use of animals.

References

1. Mylvaganam RJ, Bailey JI, Sznajder JI, et al. Recovering from a pandemic: pulmonary fibrosis after SARS-CoV-2 infection. Eur Respir Rev 2021;30:210194.
2. Sgalla G, Comes A, Lerede M, et al. COVID-related fibrosis: insights into potential drug targets. Expert Opin Investig Drugs 2021;30:1183-95.
3. Duitman J, van den Ende T, Spek CA. Immune Checkpoints as Promising Targets for the Treatment of Idiopathic Pulmonary Fibrosis? J Clin Med 2019;8:1547.
4. Kolahian S, Fernandez IE, Eickelberg O, et al. Immune Mechanisms in Pulmonary Fibrosis. Am J Respir Cell Mol Biol 2016;55:309-22.
5. Suliman HB, Healy Z, Zobi F, et al. Nuclear respiratory factor-1 negatively regulates TGF-β1 and attenuates pulmonary fibrosis. iScience 2021;25:103535.
6. Du J, Zhu Y, Meng X, et al. Atorvastatin attenuates paraquat poisoning-induced epithelial-mesenchymal transition via downregulating hypoxia-inducible factor-1 alpha. Life Sci 2018;213:126-33.
7. Li C, Hu D, Xue W, et al. Treatment Outcome of Combined Continuous Venovenous Hemofiltration and Hemoperfusion in Acute Paraquat Poisoning: A Prospective Controlled Trial. Crit Care Med 2018;46:100-7.
8. Sun H, Jiang Y, Song Y, et al. The MUC5B Mucin Is Involved in Paraquat-Induced Lung Inflammation. Oxid Med Cell Longev 2020;2020:7028947.
9. Dinis-Oliveira RJ, Duarte JA, Sánchez-Navarro A, et al. Paraquat poisonings: mechanisms of lung toxicity, clinical features, and treatment. Crit Rev Toxicol 2008;38:13-71.
10. Cui Y, Xin H, Tao Y, et al. Arenaria kansuensis attenuates pulmonary fibrosis in mice via the activation of Nrf2 pathway and the inhibition of NF-kB/TGF-beta1/Smad2/3 pathway. Phytother Res 2021;35:974-86.
11. Yang L, Liu G, Li X, et al. Small GTPase RAB6 deficiency promotes alveolar progenitor cell renewal and attenuates PM2.5-induced lung injury and fibrosis. Cell Death Dis 2020;11:827.
12. Hinz B. The role of myofibroblasts in wound healing. Curr Res Transl Med 2016;64:171-7.
13. Ramazani Y, Knops N, Elmonem MA, et al. Connective tissue growth factor (CTGF) from basics to clinics. Matrix Biol 2018;68-69:44-66.
14. Brigstock DR. Connective tissue growth factor (CCN2, CTGF) and organ fibrosis: lessons from transgenic animals. J Cell Commun Signal 2010;4:1-4.
15. Kim H, Son S, Ko Y, et al. CTGF regulates cell proliferation, migration, and glucose metabolism through activation of FAK signaling in triple-negative breast cancer. Oncogene 2021;40:2667-81.
16. Yang H, Huang Y, Chen X, et al. The role of CTGF in the diabetic rat retina and its relationship with VEGF and TGF- (2) , elucidated by treatment with CTGFsiRNA. Acta Ophthalmol 2010;88:652-9.
17. Johnson BG, Ren S, Karaca G, et al. Connective Tissue Growth Factor Domain 4 Amplifies Fibrotic Kidney Disease through Activation of LDL Receptor-Related Protein 6. J Am Soc Nephrol 2017;28:1769-82.
18. Burgy O, Königshoff M. The WNT signaling pathways in wound healing and fibrosis. Matrix Biol 2018;68-69:67-80.
19. Yang Z, Sun Z, Liu H, et al. Connective tissue growth factor stimulates the proliferation, migration and differentiation of lung fibroblasts during paraquat-induced pulmonary fibrosis. Mol Med Rep 2015;12:1091-7.
20. Velagacherla V, Mehta CH, Nayak Y, et al. Molecular pathways and role of epigenetics in the idiopathic pulmonary fibrosis. Life Sci 2022;291:120283.
21. Jarzebska N, Karetnikova ES, Markov AG, et al. Scarred Lung. An Update on Radiation-Induced Pulmonary Fibrosis. Front Med (Lausanne) 2021;7:585756.
22. Pakshir P, Hinz B. The big five in fibrosis: Macrophages, myofibroblasts, matrix, mechanics, and miscommunication. Matrix Biol 2018;68-69:81-93.
23. Bugg D, Bailey LRJ, Bretherton RC, et al. MBNL1 drives dynamic transitions between fibroblasts and myofibroblasts in cardiac wound healing. Cell Stem Cell 2022;29:419-433.e10.
24. Wu Q, Jiao B, Gui W, et al. Long non-coding RNA SNHG1 promotes fibroblast-to-myofibroblast transition during the development of pulmonary fibrosis induced by silica particles exposure. Ecotoxicol Environ Saf 2021;228:112938.

25. Vanstapel A, Goldschmeding R, Broekhuizen R, et al. Connective Tissue Growth Factor Is Overexpressed in Explant Lung Tissue and Broncho-Alveolar Lavage in Transplant-Related Pulmonary Fibrosis. Front Immunol 2021;12:661761.
26. Soundararajan R, Varanasi SM, Patil SS, et al. Lung fibrosis is induced in ADAR2 overexpressing mice via HuR-induced CTGF signaling. FASEB J 2022;36:e22143.
27. Xu X, Dai H, Geng J, et al. Rapamycin increases CCN2 expression of lung fibroblasts via phosphoinositide 3-kinase. Lab Invest 2015;95:846-59. Erratum in: Lab Invest 2021;101:136-7.
28. Yang X, Ma L, Wei R, et al. Twist1-induced miR-199a-3p promotes liver fibrosis by suppressing caveolin-2 and activating TGF-β pathway. Signal Transduct Target Ther 2020;5:75.
29. Tsunoda T, Kakinuma S, Miyoshi M, et al. Loss of fibrocystin promotes interleukin-8-dependent proliferation and CTGF production of biliary epithelium. J Hepatol 2019;71:143-52.
30. Falke LL, Goldschmeding R, Nguyen TQ. A perspective on anti-CCN2 therapy for chronic kidney disease. Nephrol Dial Transplant 2014;29 Suppl 1:i30-7.
31. Rooney B, O'Donovan H, Gaffney A, et al. CTGF/CCN2 activates canonical Wnt signalling in mesangial cells through LRP6: implications for the pathogenesis of diabetic nephropathy. FEBS Lett 2011;585:531-8.
32. Yang Z, Sun L, Nie H, et al. Connective tissue growth factor induces tubular epithelial to mesenchymal transition through the activation of canonical Wnt signaling in vitro. Ren Fail 2015;37:129-35.
33. Yanagihara T, Tsubouchi K, Gholiof M, et al. Connective-Tissue Growth Factor Contributes to TGF-β1-induced Lung Fibrosis. Am J Respir Cell Mol Biol 2022;66:260-70.
34. Klay D, van der Vis JJ, Roothaan SM, et al. Connective Tissue Growth Factor Single Nucleotide Polymorphisms in (Familial) Pulmonary Fibrosis and Connective Tissue Disease Associated Interstitial Lung Disease. Lung 2021;199:659-66.
35. Hu HH, Cao G, Wu XQ, et al. Wnt signaling pathway in aging-related tissue fibrosis and therapies. Ageing Res Rev 2020;60:101063.
36. Hiyama A, Morita K, Sakai D, et al. CCN family member 2/connective tissue growth factor (CCN2/CTGF) is regulated by Wnt-β-catenin signaling in nucleus pulposus cells. Arthritis Res Ther 2018;20:217.
37. Dorn LE, Petrosino JM, Wright P, et al. CTGF/CCN2 is an autocrine regulator of cardiac fibrosis. J Mol Cell Cardiol 2018;121:205-11.
38. Sgalla G, Franciosa C, Simonetti J, et al. Pamrevlumab for the treatment of idiopathic pulmonary fibrosis. Expert Opin Investig Drugs 2020;29:771-7.
39. Richeldi L, Fernández Pérez ER, Costabel U, et al. Pamrevlumab, an anti-connective tissue growth factor therapy, for idiopathic pulmonary fibrosis (PRAISE): a phase 2, randomised, double-blind, placebo-controlled trial. Lancet Respir Med 2020;8:25-33.
40. Barbe MF, Hilliard BA, Amin M, et al. Blocking CTGF/CCN2 reduces established skeletal muscle fibrosis in a rat model of overuse injury. FASEB J 2020;34:6554-69.

(English Language Editor: L. Huleatt)

Cite this article as: Yang Z, Wang M, Cao L, Liu R, Ren Y, Li L, Zhang Y, Liu C, Zhang W, Nie S, Sun Z. Interference with connective tissue growth factor attenuated fibroblast-to-myofibroblast transition and pulmonary fibrosis. Ann Transl Med 2022;10(10):566. doi: 10.21037/atm-22-1397

